Supporting Information

1. Evolution of Scattering Intensities with Time at Variable Scattering Angle

In Figure S1, the evolution of scattering intensities with time is represented for a selection of scattering angles. Each scattering angle corresponds to a light guide ending on a photodiode. Saturation and overflow in such a detection channel is clearly detected as the respective intensity recording reaches a ceiling value. If overflow occurs, respective data are not considered for further evaluation of the particle parameter.

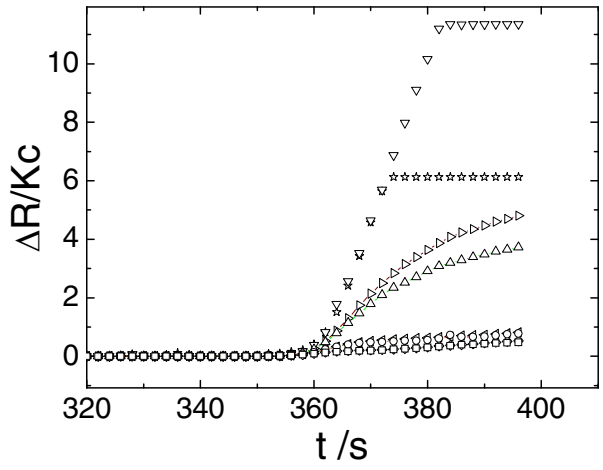

Figure S1: Scattering intensities at 8 different angles as a function of time recorded during a particle formation experiment. The $CaCO_3$ and NaOH content are 10 mM and 20 mM respectively and the temperature is T = 25°C. The symbols denote the following scattering angles: 25.87° (●); 53.19° (▷); 84.36° (◁); 113.73° (◇); -25.87° (▽); -60.06° (△); -90.10° (○); -120.16° (□).

2. Formation of ACC Particles after Mixing of Alkaline Solutions of DMC and $CaCl_2$ - Reproducibility

In order to assess reproducibility of a growth experiment based on the hydrolysis of the dimethyl carbonate (DMC), six experimental runs were collected, which were performed under identical conditions. The $CaCO_3$ content was 10 mM and the NaOH concentration was 20 mM providing equal molar concentrations of the OH^- ions and the methyl ester residues. The increase of particle mass and particle size with growth time is represented in **Figure S2 and S3**. The growth curves lead to induction times t_{ind} by extrapolating weight averaged mass values M_w to zero. Data are represented in **Table S1**. Consideration of all six values result in

an averaged value of t_{ind} = 354 s ± 4 s. The resulting correlations between size and mass are graphically represented in **Figure S4**. They follow a power law of $R_g \sim M_w^{\alpha}$. The values for the exponent α are summarized in **Table S1**. Two growth experiments exhibited slightly larger size values for which we do not have an explanation yet. Therefore, we performed three more growth runs under identical conditions (not shown here), which exactly reproduced experiments 2-4 and 6. Data provide an average value for the exponent of α = 0.161 ± 0.01. The standard deviation of α from a single growth experiment is 0.024, which corresponds to an uncertainty of 115%. In the light of such a narrow regime available for such a correlation, reproducibility of the exponent is considered to be good. Particle scattering curves from all six growth experiments, normalized to the respective particle size are compared with model curves of monodisperse rods[1], coils[2] and spheres[3] in **Figure S5**. The particle scattering factors are close to the curve of a monodisperse sphere. Curves coincide, independent of time and experiment.

Table S1: Characteristic parameters of six experiments performed under identical conditions. The $CaCO_3$ and NaOH content in all cases are 10 mM and 20 mM respectively and the temperature is T = 25°C. The symbols refer to Figures S2-S4.

	exponent α of $R_g \sim M_w^{\alpha}$	induction time / s $t_{ind} = \lim_{M_w \to 0} t$
experiment 1 (□)	0.148	356
experiment 2 (○)	0.144	355
experiment 3 (△)	0.187	354
experiment 4 (▽)	0.193	338
experiment 5 (◇)	0.135	367
experiment 6 (▷)	0.159	351
mean value	**0.161**	**354**
standard deviation of single experiment	0.024	10
standard deviation of mean value	0.01	4

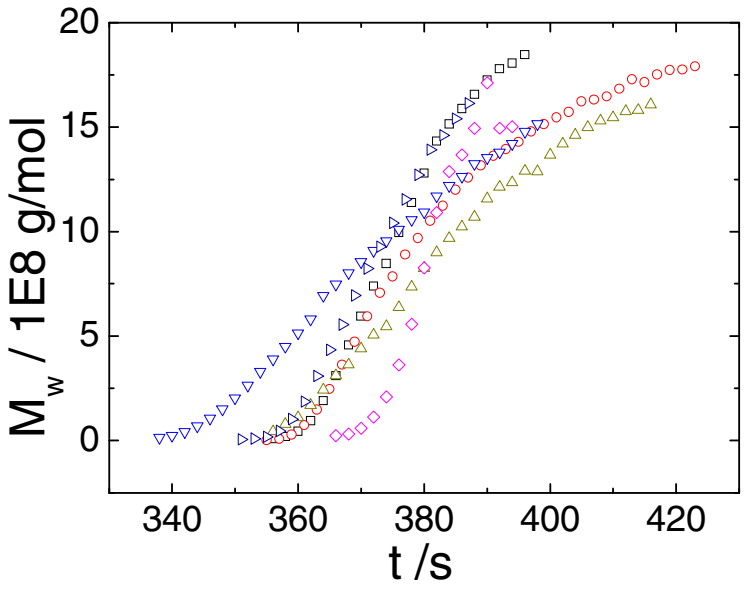

Figure S2: Increase of the weight averaged particle mass for six growth experiments initiated by ester hydrolysis under identical conditions. The $CaCO_3$ and NaOH content in all cases is 10 mM and 20 mM respectively and the temperature is T = 25°C. The symbols refer to the experiment numbers listed in **Table S1**.

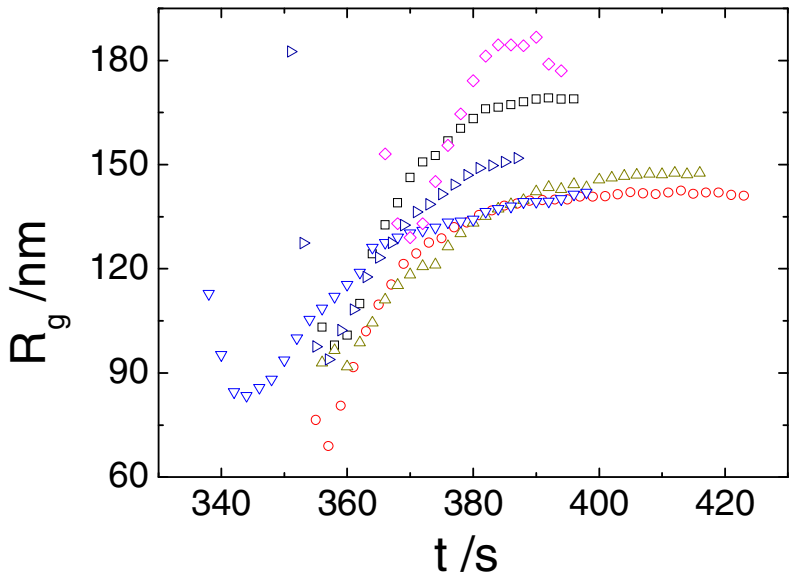

Figure S3: Increase of the square root of the z-averaged squared radius of gyration for six growth experiments initiated by ester hydrolysis under identical conditions. The $CaCO_3$ and NaOH content in all cases is 10 mM and 20 mM respectively and the temperature is T = 25°C. The symbols refer to the experiment numbers listed in **Table S1**.

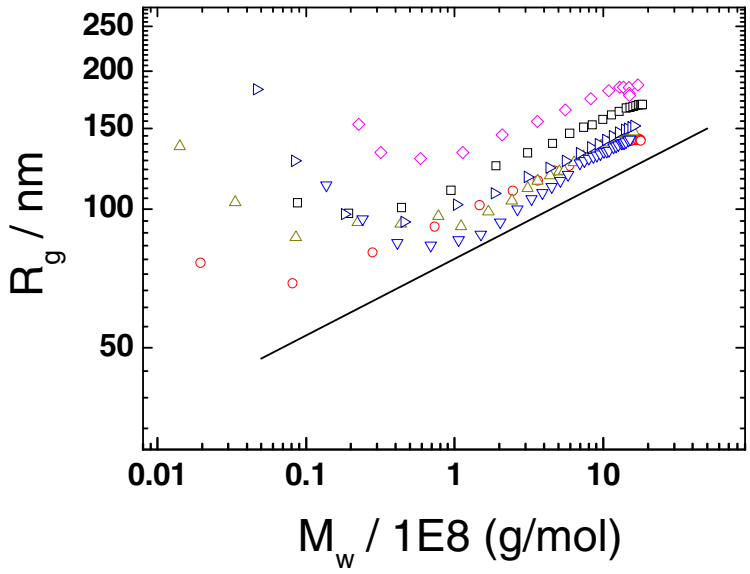

Figure S4: Correlation between particle size and particle mass for six different growth experiments initiated by ester hydrolysis under identical conditions. The $CaCO_3$ and NaOH content in all cases is 10 mM and 20 mM respectively and the temperature is T = 25°C. The symbols refer to the experiment numbers listed in **Table S1**. Power laws within experimental uncertainty obey an exponent of 1/6 indicated by the straight line.

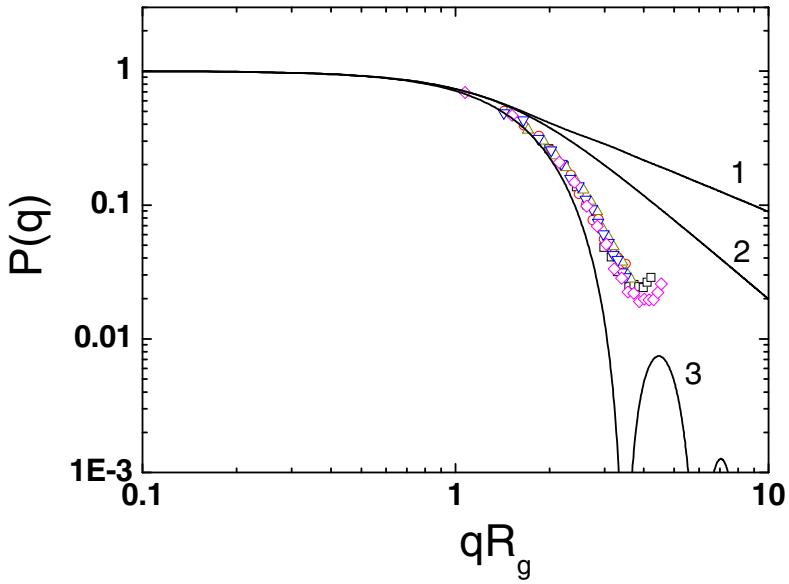

Figure S5: Particle scattering curves normalized to the radius of gyration R_g of the particles from the growth experiments summarized in Table S2 compared with model curves for a monodisperse rod[1] (1), coil[2] (2) and sphere[3] (3). All curves are recorded within a narrow time regime of 380 s < t < 400s. The symbols indicate: experiment 1 at 388 s (□); experiment 2 at 391 s (○); experiment 3 at 396 s (Δ); experiment 4 at 391 s (▽); experiment 5 at 382 s (◇).

3. Comparison of Scattering Curves of ACC Particles Induced via Hydrolysis of DMC at Variable NaOH Content

Growth experiments with [$CaCl_2$] = [DMC] = 10 mM were performed at T = 25°C and at variable NaOH concentration. The experiment at [NaOH] = 20 mM corresponds to experiment 6 in **Table S1**. **Figure S6** demonstrates that the normalized formfactors recorded at different growth times overlay if selected from a single growth experiment. Therefore the process is considered to produce self-similar intermediates.

Figure S7 compares particle scattering curves recorded at five different particle growth experiments. The growth experiments were performed at five different NaOH contents respectively being added initially to induce ester hydrolysis of DMC. The comparison in **Figure S7** clearly demonstrates that the particle shape does not depend on the initial NaOH content applied for the respective growth experiments.

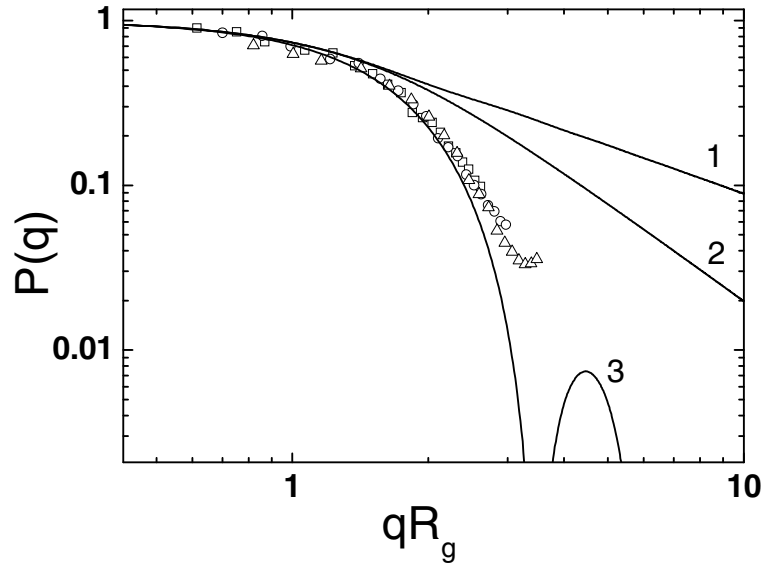

Figure S6: Particle scattering curves normalized to the radius of gyration R_g of the particles compared with model curves for a monodisperse rod[1] (1), coil[2] (2) and sphere[3] (3). The data stem from a growth experiment according to the FW-method at [NaOH] = 16 mM. The symbols indicate the following growth times: 416 s (□); 420 s (○); 428 s (Δ).

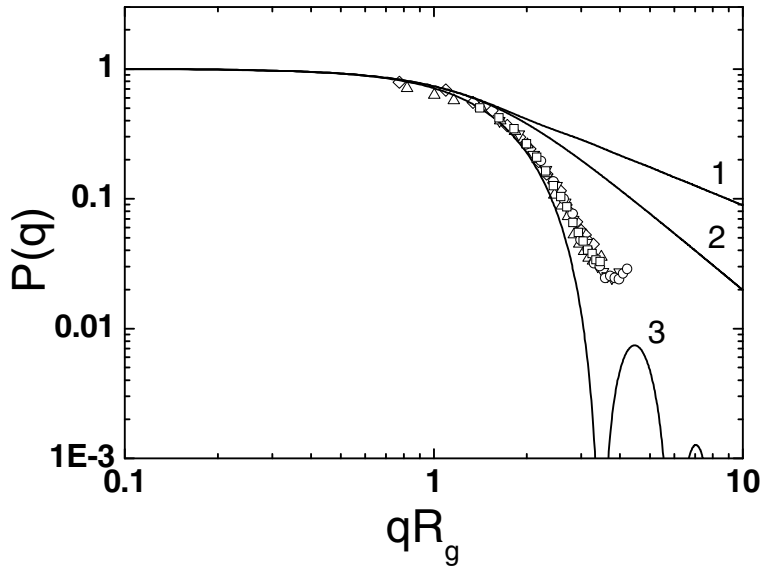

Figure S7: Particle scattering curves normalized to the radius of gyration R_g of the particles compared with model curves for a monodisperse rod[1] (1), coil[2] (2) and sphere[3] (3). The data stem from five different growth experiments induced at different initial concentrations of NaOH. The symbols indicate the following parameters: [NaOH] = 10 mM at 609 s (◇); [NaOH] = 12.5 mM at 518 s (▽); [NaOH] = 16 mM at 428 s (Δ); [NaOH] = 20 mM at 388 s (○); experiment 5 at 346 s (□).

Table S2: Characteristic parameters of experiments performed at variable initial NaOH concentrations. The $CaCO_3$ content and temperature in all cases is 10 mM 25°C respectively.

[NaOH] / mM	exponent α of $R_g \sim M_w^{\alpha}$	induction time / s $t_{ind} = \lim_{M_w \to 0} t$
25	0.184	311
20	0.159	351
16	0.178	405
12.5	0.167	472
10	0.190	556

5. Scattering Results for FW-Experiments at Variable Temperature

Figures S8 – S10 show results from a selection of growth experiments at five different temperatures in a range of 20°C ≤ T ≤ 30°C. The exponents of the correlation between the radius of gyration and the weight averaged particle mass and the induction times are summarized in **Table S3**. The experiment at 25°C corresponds to experiment 1 in **Table S1**.

Table S3: Characteristic parameters of experiments performed at variable temperatures. The $CaCO_3$ and NaOH content in all cases are 10 mM and 20 mM respectively.

temperature	exponent α of $R_g \sim M_w^{\alpha}$	induction time / s $t_{ind} = \lim_{M_w \to 0} t$
20°C	0.130	588
21°C	0.170	485
24°C	0.122	377
25°C	0.148	356
30°C	0.144	237

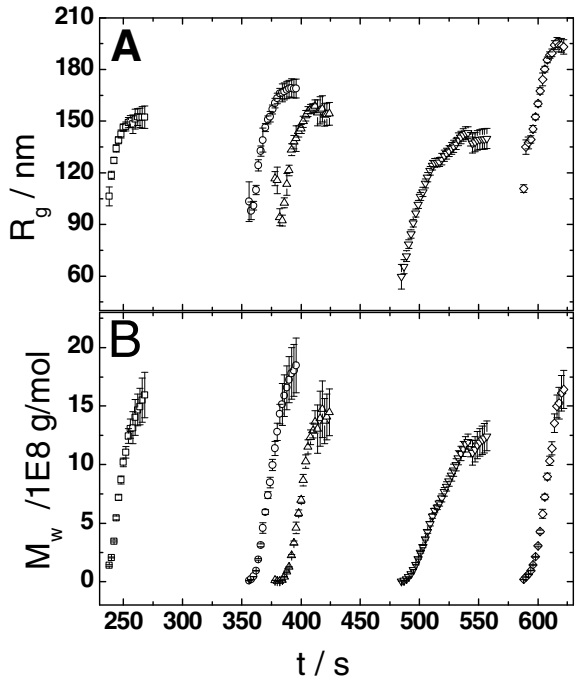

Figure S8: Aggregation experiments prepared according to the FW-method at variable temperature. The $CaCO_3$ content and the NaOH concentration in all cases was 10 mM and 20 mM respectively. Figure A shows the increase in particle mass and Figure B the increase in particle size expressed in terms of the radius of gyration. The symbols denote the following temperatures: T=20°C (◇); T = 21°C (▽); T = 24°C (△); T = 25°C (○); 30°C (□).

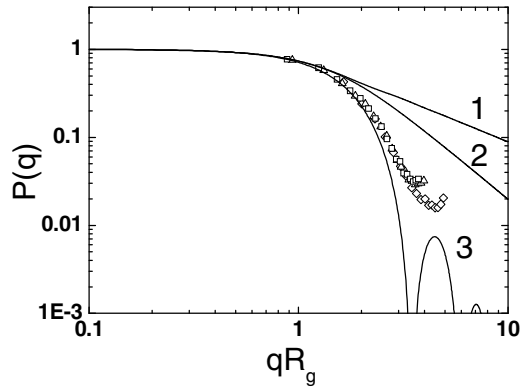

Figure S9: Particle scattering curves of aggregation runs performed with [$CaCO_3$]=10 mM and [NaOH]=20 mM at T = 20°C (◇, t=616 s), 24°C (△, t=410 s) and 30°C (□, t=254 s) respectively in comparison with model curves for a monodisperse rod[1] (1), coil[2] (2) and sphere[3] (3).

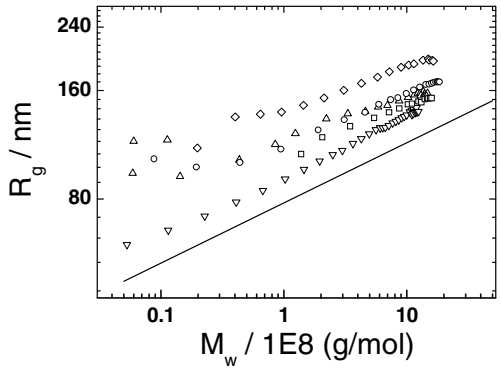

Figure S10: Correlation between particle size and particle mass at five different temperatures. The $CaCO_3$ content and the NaOH concentration in all cases was 10 mM and 20 mM respectively. The symbols denote the following temperatures: T=20°C (◇); T = 21°C (▽); T = 24°C (△); T = 25°C (○); 30°C (□). The straight line indicate an exponent of 1/6.

6. Scattering Results for FW-Experiments at Variable Salinity

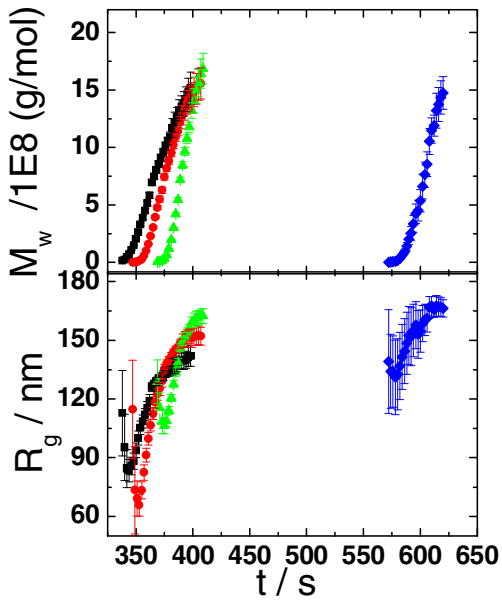

Figure S11: Aggregation experiments prepared according to the FW-method at variable NaCl concentrations at T = 25°C. The $CaCO_3$ content and the NaOH concentration in all cases was 10 mM and 20 mM respectively. The upper Figure shows the increase in particle mass and the lower Figure the increase in particle size expressed in terms of the radius of gyration. The symbols denote the following salinities: [NaCl] = 0 M, (■); [NaCl] = 0.001 M (●), [NaCl] = 0.01 M, (▲) and [NaCl] = 0.1 M, (◆).

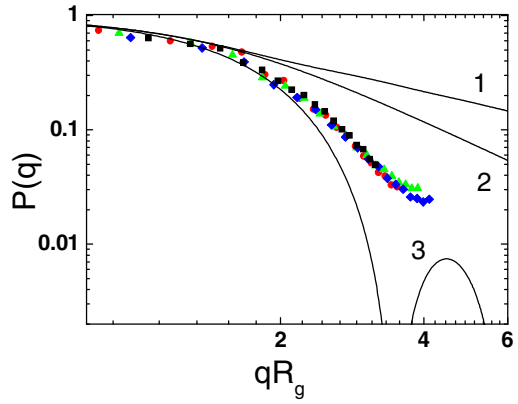

Figure S12: Particle scattering curves of the aggregation run at variable [NaCl] (see also Figure 13) in comparison with model curves for a monodisperse rod[1] (1), coil[2] (2) and sphere[3] (3). The symbols indicate the aggregation time and NaCl concentration: 364 s at 0 M (■); 402 s at 0.001 M (●); 403 s at 0.01 M (▲) and 620 s at 0.1 M (◆)

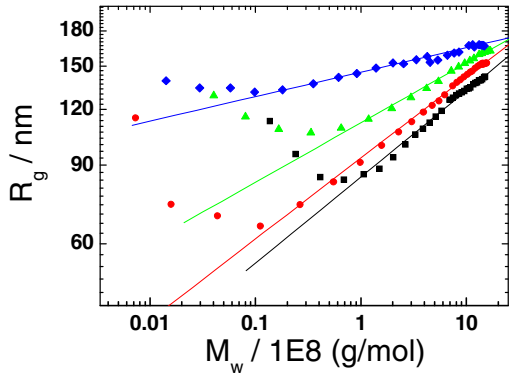

Figure S13: Correlation between particle size and particle mass at variable NaCl concentration. The $CaCO_3$ content and the NaOH concentration in all cases was 10 mM and 20 mM respectively. The resulting exponents are 0.20 ([NaCl] = 0 M, ■); 0.19 ([NaCl] = 0.001 M ●), 0.18 ([NaCl] = 0.01 M ▲), and 0.055 ([NaCl] = 0.1 M ◆).

Table S4: Characteristic parameters of experiments performed at variable [NaCl] contents and at T = 25°C. The $CaCO_3$ and NaOH content in all cases are 10 mM and 20 mM respectively and the temperature is T = 25°C. The experiment at 0 M [NaCl] corresponds to experiment 4 in Table S2.

[NaCl] / M	exponent α of $R_g \sim M_w^{\alpha}$	induction time / s $t_{ind} = \lim_{M_w \to 0} t$
0	0.193	338
0.001	0.182	350
0.01	0.133	370
0.1	0.055	572

7. Kinetic Equations for the Hydrolysis of DMC

Formation of the carbonate ions by hydrolysis of the DMC according to eq(20) (in the manuscript) causes a variation of the CO_3^{2-} and OH^- concentration. The concentrations of all species involved in the ester hydrolysis are interrelated by four relationships

$$[DMC] = [DMC]_0 - \Delta_{DMC} \quad \text{(S7-1a)}$$

$$[OH^-] = [OH^-]_0 - [MeOH] \quad \text{(S7-1b)}$$

$$[MeOH] = 2\Delta_{DMC} - [MMC^-] \quad \text{(S7-1c)}$$

$$[CO_3^{2-}] = \Delta_{DMC} - [MMC^-] \quad \text{(S7-1c)}$$

With Δ_{DMC} the dimethyl carbonate, consumed by ester hydrolysis, MeOH the methanol and MMC^- the mono-methyl-ester of the carbonic acid as the intermediate of the hydrolysis.

Initial concentrations of all species are fixed by the four boundary conditions

$$[DMC]_0 = 10 \text{ mM} \quad \text{(S7-2a)}$$

$$[OH^-]_0 = 25 \text{ mM, } 20 \text{ mM, } 16 \text{ mM, } 12.5 \text{ mM and } 10 \text{ mM respectively} \quad \text{(S7-2b)}$$

$$[MMC^-]_0 = 0 \quad \text{(S7-2c)}$$

$$[CO_3^{2-}]_0 = 0 \quad \text{(S7-2d)}$$

$$[MeOH] = 0 \quad \text{(S7-2e)}$$

Representation of $[OH^-]$ and $[CO_3^{2-}]$ as a function of reaction time t is based on a time axis, which is divided into increments $\Delta t = 1$ s with $t = i\Delta t$. The axis extends over $0 \leq i \leq 5000$.

$$[DMC]_{i+1} = [DMC]_i - k_1[DMC]_i[OH^-]_i 8t \quad \text{(S7-3a)}$$

$$[OH^-]_{i+1} = [OH^-]_i - k_1[DMC]_i[OH^-]_i 8t - k_2[MMC^-]_i[OH^-]_i 8t \qquad \text{(S7-3b)}$$

$$[CO_3^{2-}]_{i+1} = [CO_3^{2-}]_i + k_2[MMC^-]_i[OH^-]_i 8t \qquad \text{(S7-3c)}$$

The differential equations eq (S7-3) require the rate constants k_1 and k_2 first introduced in eq (20) of the manuscript. Both constants were determined experimentally by Faatz[4] and are summarized as follows

$$k_1 = 0.113 \text{ L(mol s)}^{-1} \qquad \text{independent of } [OH^-]_0 \qquad \text{(S7-4)}$$

$$k_2 = a + b \cdot t \qquad \text{(S7-5)}$$

The coefficients a and b in eq (S7-5) depend on the initial OH^- concentration $[OH^-]_0$ according to

$$a = -0.365 + 25.623\ [OH^-]_0\ , \quad [OH^-]_0 \leq 0.014 \text{ mol/L} \qquad \text{(S7-6a)}$$

$$a = 0.0514 + 2.6\ [OH^-]_0\ , \qquad [OH^-]_0 > 0.014 \text{ mol/L} \qquad \text{(S7-6b)}$$

$$\ln(b) = -6.021 - 167.01(\text{L/mol}) \cdot [OH^-]_0 \qquad \text{(S7-7)}$$

Alternatively, the $[OH^-]_0$ dependence of a can be represented by an empirical fit of

$$a = 0.0894 - 0.00168 / [OH^-]_0 \qquad \text{(S7-6c)}$$

Application of eqs (S7-6a) and (S7-6b) certainly provides a better accuracy if data are considered with either $[OH^-]_0 > 14$ mM or $[OH^-]_0 < 10$ mM. However, in the transition regime of 10 mM < $[OH^-]_0$ < 14 mM, relationship (S7-6c) has the advantage of following a smooth trend without any kink. Thus eq (S7-6c) or alternatively eq (S7-6a) together with (S7-6b) has been applied to describe the variation of k_2 over the whole regime of $[OH^-]_0$ investigated in the present work. For the impact of temperature and salinity on the DMC hydrolysis, eq (S7-6b) has been used because the initial OH concentration was always above 14 mM.

By establishing *a* and b with eqs (S7-6) and (S7-7) respectively, the rate constant k_2 in eq (S7-5) reads

$$k_2 = a([OH^-]_0) + b([OH^-]_0)\, i\Delta t \qquad \text{(S7-8)}$$

with $(L/(mol))^2/s$ and $(L/(mol \cdot s))^2$ the dimensions of a and b respectively in eqs (S7-5), (S7-6) and (S7-8). Negative values for k_2 may occur at initial times close to the onset of hydrolysis. These are unphysical and were set to zero.

For temperature dependent kinetics, we fixed the initial concentration of OH^- $[OH^-]_0$ = 20 mM. Rate constants were determined experimentally by Faatz et al.[4] and used in the following way. The constant k_1 corresponds to eq (S7-4), independent of temperature.

The rate constant k_2 depends on temperature. At an initial OH^- concentration of 20 mM this temperature dependence is considered by a temperature variation of b according to

$$\ln\{b([OH^-]_0 = 20mM;\, T°C)\} = 34.47 - 13068.94*(1/T°C) \qquad \text{(S7-9)}$$

The temperature dependence of *a* turned out to be weak[4] and negligible within a range of room temperature $\pm$ 5°C. Yet, an estimation for *a* in a limited regime around room temperature can be performed under the assumption that *a* follows the same trend as b.

$$a(T°C) = a(25°C) * b([OH^-]_0 = 20mM;\, T°C)/b([OH^-]_0 = 20mM;\, 25°C) \qquad \text{(S7-10)}$$

The temperature dependence of the solubility product of ACC is approximated according to

$$-\log\{L_{ACC}/M^2\} = 6.1987 + 0.005336(T-273K) + 0.0001096(T-273K)^2 \qquad \text{(S7-11)}$$

based on the work of Brecevic & Nielsen[5] and according to

$$\log\{L_{ACC}/M^2\} = (1247.0/T) - 10.224 \qquad \text{(S7-12)}$$

based on the work of Adams et al[6].

References

1. Neugebauer, T. *Ann. Phys.* . **1943**, *434*, 509-533

2. Debye, P. *J. Phys. Colloid Chem.* **1947**, *51*, 18-32

3. Rayleigh, L. *Proc. R. Soc. London, Ser. A* **1914**, *90*, 219-225

4. Faatz, M. *Kontrollierte Fällung von amorphem Calciumcarbonat durch homogene Carbonatfreisetzung*, Dissertation Mainz **2005**

5. Brecevic, L. ; Nielsen, A. E. *J. Cryst. Growth* **1989**, *98*, 504-510

6. Clarkson, J. R. ; Price, T. J. ; Adams, C. J. *J. Chem. Soc. Faraday Trans.* **1992**, *88*, 243-249